AIAA 99-0672

Periodic Excitation for Jet Vectoring and Enhanced Spreading

LaTunia G. Pack and Avi Seifert

NASA Langley Research Center

Hampton, VA

37th AIAA Aerospace Sciences Meeting and Exhibit

January 11-14, 1999/ Reno, NV

Periodic Excitation for Jet Vectoring and Enhanced Spreading

LaTunia G. Pack* and Avi Seifert**
Flow Modeling and Control Branch
NASA Langley Research Center, Hampton, VA 23681

Abstract

The effects of periodic excitation on the evolution of a turbulent jet were studied experimentally. A short, wide-angle diffuser was attached to the jet exit and excitation was introduced at the junction between the jet exit and the diffuser inlet. The introduction of high amplitude periodic excitation at the jet exit enhances the mixing and promotes attachment of the jet shear-layer to the diffuser wall. Vectoring is achieved by applying the excitation over a fraction of the circumference of the circular jet, enhancing its spreading rate on the excited side and its tendency to reattach to that side. Static deflection studies demonstrate that the presence of the wide-angle diffuser increases the effectiveness of the added periodic momentum due to a favorable interaction between the excitation, the jet shear-layer and the diffuser wall. This point was further demonstrated by the evolution of a wave packet that was excited in the jet shear-layer. Strong amplification of the wave packet was measured with a diffuser attached to the jet exit. The turbulent jet responds quickly (10-20 msec) to step changes in the level of the excitation input. The response scales with the jet exit velocity and is independent of the Reynolds number. Jet deflection angles were found to be highly sensitive to the relative direction between the excitation and the jet flow and less sensitive to the excitation frequency. The higher jet deflection angles were obtained for a diffuser length of about two diameters and for diffusers with half-angles greater than 15 degrees.

Nomenclature

A_{jet}	jet cross-section area, πr^2
A_{slot}	active slot area, $\pi h(2r+h)/4$
$<c_\mu>$	periodic momentum coefficient, $J'/(\rho A_{jet} U_e^2)$
D	jet diameter, 39mm
F^+	reduced frequency, fL/U_e
f	excitation frequency [Hz]
h	slot width or height, 1mm
J'	periodic momentum at slot exit, $\rho A_{slot} u'^2_{slot}$
K	1000
L	distance from jet exit to diffuser exit, measured along diffuser wall
p	pressure
r	jet radius, 19.5mm
Re_D	Reynolds number based on diameter, $U_e D/\nu$
RMS	root mean square of fluctuating value
S_{tD}	Strouhal number, fD/U_e
$S_{t\theta}$	Strouhal number, $f\theta/U_e$
t	time
U	jet mean velocity
U_c	wave packet convection velocity
u'	root mean square of the velocity fluctuations
ν	kinematic viscosity
V	y velocity component
x	axial direction, x=0 at jet exit and diffuser inlet
y	vertical direction, y=0 at jet centerline
y_c	jet center of momentum
z	horizontal direction, z=0 at jet centerline
δ	jet deflection angle, [deg]
ρ	density
ø	diffuser half-angle, [deg]
θ	jet 2-dimensional shear-layer momentum thickness

Subscripts

d	de-rectified
e	conditions at jet exit
i	index denoting z location
slot	condition at slot exit
plane	profiles of an entire jet cross-section
profile	jet profile at z/D=0.0

Terminology

X-diffuser	streamwise excitation diffuser
R-diffuser	cross-stream excitation diffuser
Baseline	No control, f=$<c_\mu>$=0.0

---

* Research engineer, Flow Modeling and Control Branch.
** NRC researcher, on leave from Tel-Aviv University, member AIAA.

1. Introduction

Turbulent jets are of significant engineering relevance for aerospace and mechanical applications (jet engines, combustion chambers, etc.) and to the environment (chimney stacks). As such, they have been extensively investigated over the last few decades. Controlled excitation was initially used in order to clarify the importance of coherent structures on the evolution of transitional and turbulent jets[1,2]. Research efforts were devoted to understanding the importance of coherent structures in noise generation and jet spreading. Controlled, far field, acoustic excitation was used in most of these studies to generate the jet coherent structures, owing to the strong receptivity of the jet lip. The limitations of acoustic excitation (power requirements, weight, applicability, and efficiency) led researchers to examine other methods for jet flow control. These methods include cross-stream blowing[3], counter-flow[4,5,6], self-excited resonance tubes[7] and high amplitude periodic excitation[8]. Davis[3] introduced cross-stream blowing through two circular tubes positioned on each side of the jet exit. It was shown that the radial introduction of steady momentum enhanced mixing for secondary jet momentum coefficients lower than 0.56%. For higher momentum coefficients, a mean flow distortion was generated. Vectoring was not seen since both control jets were always operated simultaneously.

Strykowski and Wilcoxin[4] attached a diffuser 1.0 to 2.25 jet diameters long, to a low speed, circular jet and applied suction around the jet circumference. The application of suction modifies the jet exit velocity profile and turns it absolutely unstable for suction velocities greater than 31.5% of the jet centerline velocity[9]. Enhanced mixing or vectoring could be achieved depending on the fraction of the jet circumference to which suction was applied. Thrust vectoring was demonstrated at a Mach number of 2.0, using the jet-suction diffuser arrangement when suction was applied over a fraction of the circumference of a circular jet[5] or along one wall of a rectangular jet[6]. Jet deflection angles were determined by flow visualization. Since the diffuser angles were relatively small, a bi-stable situation was encountered because the jet had a tendency to naturally reattach to the diffuser walls.

Raman and Cornelius[7] used a resonance tube with openings on opposite sides of a low speed rectangular jet to generate alternating suction and blowing with 180˚ phase shift between the openings. This generated a flapping mode that enhanced the mixing of the primary jet flow. Smith and Glezer[8] used a narrow excitation slot positioned close to the exit of a high aspect-ratio low-speed rectangular primary jet. The interaction between the jet and the high frequency and high amplitude excitation vectored the primary jet. It is not known if the primary jet was laminar, transitional, or turbulent. The magnitude of the fluctuating excitation momentum at the slot exit was not specified. The authors concluded that the mechanism responsible for the jet deflection was a low pressure region generated by the excitation between the primary jet and the excitation slot.

The aim of the present investigation is vectoring and enhanced spreading of a circular, turbulent jet. The mechanism used for vectoring the jet is zero-mass-flux periodic excitation. Periodic excitation is used due to its demonstrated ability to effectively control separation on airfoils. Experiments performed on a variety of airfoils, over a large range of Reynolds and Mach numbers, indicate that periodic excitation can be used to effectively delay turbulent boundary layer separation and reattach separated flows[10,11,12]. The introduction of periodic excitation slightly upstream of the boundary layer separation location enhances mixing between the high momentum fluid away from the surface and the low momentum fluid near the surface. Periodic excitation is significantly more efficient than steady suction and two orders of magnitude more efficient than steady blowing at controlling separation[10,11,12]. This method can be applied to a turbulent jet by attaching a short, wide-angle diffuser to the jet exit and perturbing the separated shear-layer at the inlet to the diffuser.

The three main advantages of using periodic excitation for jet flow control are:

1) the potential weight reduction of a thrust vectoring system (mechanical thrust vectoring vanes account for as much as 30% of the weight of jet engines),
2) the ability to change the aerodynamic forces and moments quickly without generating prohibitive inertial loads on the structure, and
3) the demonstrated superior efficiency of the method compared to steady suction or blowing.

The present paper demonstrates the enhanced controllability of a turbulent jet when a short, wide-angle diffuser is attached at the jet exit and periodic excitation is introduced at the juncture between the jet exit and the diffuser inlet. The results of a preliminary parametric study are presented and show how jet deflection angles were affected by the diffuser geometry (i.e. diffuser length and diffuser half-angle) as well as by variations in the control inputs (such as excitation frequency, its periodic momentum, and the relative orientation of the

excitation). The response of the jet to generic control inputs was also investigated. The relationship between the present control strategy and the flow stability was examined in order to shed light on how the excitation interacts with the jet flow and the diffuser walls. In the present study we do not attempt to compare the effectiveness of this method to other jet control methods. Such a comparison would involve the definition and use of common terminology for input parameters and their effectiveness. To date, most published results do not provide enough details to make this comparison.

2. Experiment Set-up

2.1 Jet

The jet facility consists of a DC fan connected to a 76.2 mm diameter settling chamber, followed by a 3.15:1 contraction and a straight aluminum pipe with an inside diameter of 38mm and an outside diameter of 40mm. The thickness of the pipe wall, at the jet exit, was machined to bring it gradually to 0.5mm, in order to reduce the gap between the jet flow and the excitation slot. The jet exit diameter is therefore 39mm (Figs. 1a and 1b). The jet was surrounded by a 1mm wide segmented slot. Each segment of the slot was connected to a cavity allowing independent excitation of every 45˚ of the jet circumference. Although steady blowing and suction could be introduced through the slot, the results presented here are for zero-mass-flux periodic excitation (i.e. no steady component). The excitation was introduced through the slot surrounding the upper 90˚ of the jet circumference, as shown in Figures 1a and 1b. The divider between the two cavities connected to the excited region of the slot was removed, resulting in one continuous cavity over a 90˚ region of the jet. Trip grit (#36) was placed inside the aluminum pipe 200 mm from the jet exit to ensure that the flow at the jet exit was turbulent over the velocity range of interest (8 m/s- 18 m/s).

2.2 Diffusers

A short, wide-angle diffuser could be attached to the exit of the jet. The effect of diffuser length on jet deflection angle was studied by testing diffusers of length, L=0.58D, 1.0D and 1.85D. Diffusers with half-angles of ø=30˚ were used to study the effect of diffuser length. The effect of diffuser half-angle on jet deflection angle was also examined. Diffusers with half-angles of ø=15˚, 22.5˚, and 30˚ were tested. For the diffuser half-angle study, the diffuser length remained fixed at L=0.58D. The ø=30˚, L=1.85D diffuser was designed such that periodic excitation could be introduced in the streamwise and cross-stream direction. The diffuser that introduces the excitation in the stream-wise direction will be referred to as the X-diffuser and the diffuser that introduces the excitation in the cross-stream direction will be referred to as the R-diffuser.

2.3 Actuator

A Piezo-electric actuator, that resonated near 700Hz, was used to produce the periodic excitation. The velocity fluctuations, u', exiting the slot were measured using a hot-wire positioned at the slot exit. Since hot-wires can not sense flow direction, the velocities obtained at the slot exit, in the absence of jet flow, had to be de-rectified using the procedure described in Ref. 12. The maximum u' of the actuator, u'_{max}, when operated at 700 Hz using the X-diffuser, is about 18 m/s. u'_{max} is about 10% lower when the R-diffuser is used. When the actuator operated at 300Hz, using the X-diffuser, u'_{max}, was about 7m/s. The hot-wire measurements were used to determine the relationship between the input RMS voltage to the actuator and the resultant velocity fluctuations. The linear relationship that was found between the actuator input RMS voltage and u' was used to determine u' when the hot-wire was removed. In addition, a dynamic pressure transducer was flush-mounted in the collar surrounding the jet to monitor the state of the actuator and serve as a phase reference (Figure 1b). The actuator did not show signs of performance degradation during four months of experiments, as indicated by the dynamic pressure transducer monitoring the actuator output and occasional calibration checks at the slot exit using a hot-wire

2.4 Instrumentation and Data Acquisition

Most of the jet flow field measurements were acquired using a single-wire hotwire. Hot-wire calibrations were performed frequently to ensure that there were no significant drifts and data repeatability was checked often. The normal data sequence, or run, included acquiring data of the jet baseline flow field before and after acquiring data of the jet controlled flow field. A check of the two baseline data sets also served as a check of the hot-wire calibration. In addition to hot-wire measurements, a small amount of data were acquired using a 5-hole probe[13].

Hot-wire and static and dynamic pressure data were acquired using a 16 bit A/D converter. The dynamic pressure data were always low-pass filtered at 2KHz and amplified prior to digitization. The sampling rate of the hot-wire and the dynamic

pressure data was either 6KHz or 12KHz, and all hot-wire data were low-pass filtered at the sampling rate divided by 2.56. The hot-wire frequency response was always better than 20KHz. The dynamic pressure transducer also has a frequency response in excess of 20KHz. The hotwire and the 5-hole probe were mounted to a three-axis traverse system. The traverse controller, the A/D converter, the hot-wire anemometer and the power supply for the DC fan were interfaced with a desktop computer. This helped simplify hot-wire calibrations and jet flow field measurements.

2.5 Experimental Uncertainty

The velocity measured with the hot-wire is accurate to within 2% of the local value. The hot-wire position (x, y, or z) is accurate to within ±0.04 mm, the Re_D is accurate to within 3% of the local value, the $<c_\mu>$ is accurate to within 20% of the local value, and the jet deflection estimates are accurate to within ±0.5˚ of the local value.

3. Discussion of Results

3.1 The Baseline Jet

3.1.1 Reynolds Number Effect

The flow field of the baseline jet was carefully documented over the Reynolds number range of interest to verify that the flow was turbulent and to assess the effect of Reynolds number, especially in the near exit region. Turbulent, Reynolds number independent flow was desired for this flow control experiment to eliminate transition effects thereby reducing the number of variables affecting the results. By tripping the flow five diameters upstream of the jet exit it was assured that the effects produced by using periodic excitation were not transition related and would be applicable to higher Reynolds numbers. The mean and fluctuating velocity profiles close to the jet exit, at x/D=0.1, are presented in Figures 2a and 2b. The shapes of the mean velocity profiles are identical over the Reynolds number range tested. The peak turbulence level in the shear-layer increases slightly as Reynolds number decreases, as shown in Figure 2b. The differences in the turbulence levels for the three Reynolds numbers could be due to the fact that the flow is not fully developed for the lowest Reynolds number, $Re_D=2.1x10^4$. The spectra of the velocity fluctuations measured at y/r=0.97 (Fig. 3), indicate slight differences in the slopes for the three Reynolds numbers. This is another indication that the flow is not fully turbulent for the lower Reynolds numbers but is Reynolds number independent for higher Reynolds numbers. The "two-dimensional" momentum thickness of the jet shear-layer, θ, at x/D=0.1 doubles between U_e=6m/s and 8m/s, indicating that transition from laminar to turbulent flow occurs. Between 8m/s and 18m/s ($Re_D=2.1x10^4$-$4.7x10^4$), the θ has a mean value of 1.68mm and varies by no more than ±3.0%

3.1.2 The effects of the attached diffuser

The flow field of the baseline jet, close to the jet exit, with and without diffusers at the exit was also carefully examined. The velocity profiles without a diffuser and with the L=1.85D X-diffuser and R-diffuser at x/D=1.6 are presented in Fig. 4. It shows that the presence of the diffuser has very little effect on the shape of the jet mean velocity profiles. The initial thickness of the jet shear-layer, θ, is about D/25 (Fig. 5). This value is significantly higher than the published values for laminar jet exit boundary layers[4] (D/200) as well as for turbulent boundary layers[14] (D/190). However, the elimination of Re_D effects seems more important for the present investigation, than allowing a closer comparison with a two-dimensional mixing-layer. A significant increase in θ occurs between the jet exit and x/D=0.2, with a diffuser present (Fig. 5). Further downstream, the jet spreads linearly for all three cases. The spreading rate of the jet shear-layer momentum thickness, dθ/dx, increases from 0.03 to 0.031 when a diffuser is placed at the jet exit (Figure 5). The values of the present dθ/dx are about 20% larger than those found by Husain and Hussain[14] for a turbulent jet at $Re_D=7.8x10^4$. The effect of the increased initial thickness of the jet shear-layer is to increase the required input momentum for a required modification (in this case jet deflection angle), based on airfoil separation control experiments. The high initial momentum thickness is also expected to reduce the most amplified frequency based on linear two-dimensional mixing layer theory. The velocity profiles in the near exit region of the jet are not self-similar, nor is the flow parallel. This indicates that linear parallel stability approaches are not applicable to this type of flow. Furthermore, the challenge here is to generate a mean flow modification that is inherently non-linear and non axis-symmetric.

3.2 General Aspects of Periodic Excitation

3.2.1 Baseline & Controlled Cross-section Planes

Hot-wire surveys of the jet flow field were made at a cross-stream plane at x/D=2.5 and $Re_D=3.1x10^4$. The baseline mean and fluctuating velocity contours are shown in Figures 6b and 6e. The circular shape of the baseline contours indicates that the flow is axis-symmetric. The maximum turbulence level of

the baseline jet is about 15% and the u' contours are also axis-symmetric. Controlled mean and fluctuating velocity contours using streamwise excitation are shown in Figure 6a and 6d. The excitation is introduced through the portion of the slot surrounding the upper quarter of the jet circumference. The flow is no longer axis-symmetric. The enhanced mixing between the excited jet and the surrounding ambient flow leads to higher flow rates on the upper side of the jet. The increased mixing causes the mean velocity contours to be elongated in the vertical, y, direction and contracted in the horizontal, x, direction compared to the baseline. The spanwise contraction indicates that the jet is also vectored due to forces exerted by the upper 90° of the diffuser wall and not only due to enhanced mixing at the upper side. The jet center of momentum shifts upward, indicating the jet flow is vectored up by about 6° (see analysis to follow). The maximum fluctuating velocity of the controlled flow using streamwise excitation (Figure 6d) is about $0.18\text{-}0.21U_e$ and has a horseshoe-like shape on the upper side of the jet.

Controlled excitation was also introduced in the cross-stream direction (Figs. 6c and 6f). This mode of high amplitude excitation results in a deflection of the jet away from the excitation slot. The jet cross section is now elongated in the spanwise direction. This type of excitation does not increase the spreading rate nor the turbulence level as much as the streamwise excitation does. Similar excitation modes were identified by Smith and Glezer[8], as the "push" and "pull" modes. As will be shown later, the presence of the diffuser at the jet exit significantly enhances the effectiveness of the streamwise excitation. Its effect on the cross-stream excitation has not been studied yet.

3.2.2 Determination of Jet Deflection Angle

Jet deflection angles were estimated from single profiles measured along the jet centerplane and from complete cross-section planes. The momentum rather than the flow rate was used since it is better related to the forces that are the purpose of the control strategy. The total momentum at a given spanwise location, z/D, was computed using

$$M_i = \int U^2 dy \qquad \text{(Eq. 1a)}$$

where U is the jet mean velocity at a given vertical, y, position in the profile and i is an index denoting the increment in the horizontal, z, direction. The data were integrated in y, over the valid range of the hot-wire calibration velocities. The center of momentum of the jet at a given spanwise location, z/D, was determined by

$$y_{c,i} = \frac{\int U^2 y dy}{\int U^2 dy} \qquad \text{(Eq. 1b).}$$

The deflection angle based on one profile measured at z/D=0 is defined as

$$\delta_{profile} = \tan^{-1}\left(\frac{y_{c,profile}}{x}\right) \qquad \text{(Eq. 2),}$$

where x is the distance from the jet exit to the measuring station. The center of momentum of the jet at a given cross-stream location, x/D, was determined using

$$y_{c,plane} = \frac{\sum_i M_i y_{c,i}}{\sum_i M_i} \qquad \text{(Eq. 3).}$$

The deflection angle based on a whole cross-section plane was determined by assuming the jet began deflecting at x/D=0.0 and computing jet deflection angle, δ_{plane}, using

$$\delta_{plane} = \tan^{-1}\left(\frac{y_{c,plane}}{x}\right) \qquad \text{(Eq. 4),}$$

where x is the distance from the jet exit to the measuring station. Although data of complete cross-section planes of the jet flow field provide a more comprehensive description of the flow, the time required to acquire profiles of the entire cross section is excessive and the amount of data is enormous. A parametric study at this pace would have been prohibitive. A comparison was made between the deflection angle, $\delta_{profile}$, computed using a single profile measured on the jet plane of symmetry, and the deflection angle, δ_{plane}, computed using the entire cross-section, in an attempt to find one profile in space that would be representative of the entire jet. Figure 7 shows the comparison between the two methods of computing jet deflection angles at various x/D locations. Most of the results are for the X-diffuser, but the filled symbols are for the R-diffuser (with the sign inverted). It is assumed that the jet center of momentum, at the jet exit, remains at y=z=0. The deflection angles computed for the X-diffuser, using single profiles and entire cross-sections, agree to within ±0.5°. The deflection angles computed for the R-diffuser (filled symbols, deflection sign inverted, Fig. 7) using a single profile and a complete plane, are also in very good agreement. For the remaining results presented in this paper, profiles measured at z/D=0.0 and x/D=2.5 are used to determine jet deflection angles. This location always corresponds to a plane of symmetry of the excited flow and enables an efficient parametric study that is conservative based on the results shown in Figure 7. The observation that the jet deflection angle decreases with x/D (Figure 7)

implies that the jet actually started to deflect about 1D upstream of the jet exit. To clarify this point, additional measurements were made using a five-hole probe[13]. This probe enables the acquisition of three velocity components and provides an independent measure of jet deflection angles. The jet deflection angles for the 5-hole probe were computed using the local flow angle

$$\delta_{5,j} = \tan^{-1}\left(V_j / U_j\right) \qquad \text{(Eq. 5a)},$$

and a weighted averaging over the entire profile in the form

$$\delta_{5,profile} = \frac{\sum_j U_j \delta_{5,j}}{\sum_j U_j} \qquad \text{(Eq. 5b)},$$

where j is an index in the vertical direction, y, and the local mean velocity, U, serves as a weighting function. Data where the local velocity, U, was greater than $0.15U_e$ were included in the average. The deflection angles obtained with the 5-hole probe are within ±0.5° of the deflection angles based on single hot-wire profiles. The close agreement verifies the validity of the present approach in defining the jet deflection angles. Furthermore, the jet deflection angles to be presented should be used as trends of the effects of the various parameters, while absolute angles should preferably be measured with a force balance.

3.3 Parametric Study

3.3.1. The effect of Reynolds number

To study the effect of Reynolds number on the evolution of the controlled jet, data were acquired at three jet speeds corresponding to Re_D=2.1x10^4, 3.1x10^4 and 4.2x10^4. Streamwise excitation with a frequency of 700Hz was used for this study. As will be shown later, the effect of the corresponding change in F^+ with Re_D is small. Figure 8 shows jet deflection angles versus periodic momentum coefficient, $<c_\mu>$, for the three Reynolds numbers tested. The jet deflection angles for the two higher Reynolds numbers are in excellent agreement, indicating weak Reynolds number dependence. At Re_D=2.1x10^4, the jet has lower deflection angles for lower $<c_\mu>$, and higher deflection angles for $<c_\mu>$ above 2%. This could be a result of the developing nature of the turbulent boundary layer upstream of the jet exit as shown for this Re_D in Fig. 2b and Fig. 3.

3.3.2 The effect of the excitation frequency

To study the effects of F^+ without varying Re_D, the actuator was operated at two frequencies, 700Hz (actuator resonance) and 300Hz, generating F^+=4.2 and F^+=1.8, respectively, and $<c_\mu>$ was gradually increased. The jet deflection angles presented in Fig. 9, indicate a very low sensitivity to forcing frequency, in the range of available parameters. An F^+=4.2 is slightly more effective than an F^+=1.8 for the range of $<c_\mu>$'s produced by the present actuator. Figure 9 also includes results obtained using the five-hole probe. These results agree very well in the shape of the mean velocity profiles (not shown) and in the resulting deflection angles (using Eq. 5). The shape of the baseline and controlled velocity profiles are also insensitive to F^+. Examination of the velocity spectra where U/U_e=0.5 (not shown), does not reveal any distinct frequencies with or without control. The power levels are almost identical below the excitation F^+ and the levels increase slightly above the excitation F^+. The lack of distinct peaks, even at the forcing frequencies, indicates that the excitation momentum was transferred to the mean flow and to smaller scales upstream of x/D=2.5. The overall behavior of the jet response at different Re_D and frequencies indicates low sensitivity to both Re_D and F^+ for this range of parameters.

3.3.3 The effect of the diffuser length

There is no consensus among researchers, regarding the relevant length scale that determines the effective forcing frequency, along with the velocity scale that is easily selected. One possibility is a local parameter based on the thickness of the shear-layer, perhaps θ, its momentum thickness. Another option is the jet diameter. These two parameters dominate the near and far field evolution of a transitional free jet, as identified by Drubka et. al.[15]. Presently, we introduce an additional length scale, the length of the diffuser. As will be shown later, the presence of the diffuser significantly enhances the effectiveness of the streamwise excitation. The effect of the diffuser length was investigated using X-diffusers with L/D =0.58, 1.0 and 1.85 corresponding to F^+=1.3, 2.3, and 4.2 respectively. F^+ was shown in the previous section to have little effect on jet deflection angles over this range. Figure 10 shows the deflection angles versus $<c_\mu>$ for the three diffuser lengths tested. The deflections measured using the L=0.58D diffuser were slightly lower than the deflections measured using the L=1.0D diffuser. The L=1.85D diffuser produced smaller deflections than the shorter diffusers at low $<c_\mu>$'s. However, for $<c_\mu>$ above 2% the longer diffuser (L=1.85D) generated higher deflection angles. It is assumed that the diffuser length plays an important role in the non-linear process leading to jet deflection, since the sensitivity to the forcing frequency is low (see Fig. 9 and Fig. 10).

The mean velocity profiles for the three diffuser lengths when $<c_\mu>$=0% and 3.2% are shown in Figure 11. The shift of the mean velocity profile for the jet with the L=1.85D diffuser on the lower side of the jet indicates some differences in the deflection mechanism for the longest diffuser. It also indicates a lower mixing in the excited shear-layer. The turbulence profiles (not shown) indicate that the jet velocity fluctuation levels for the L=1.85D diffuser are higher in both shear-layers and lower in the core of the jet, compared to the turbulence levels found for the shorter diffusers.

3.3.4 The effect of the diffuser half-angle

The effect of the diffuser half-angle, ø, was studied using X-diffusers with half-angles, ø=15˚, 22.5˚, and 30˚, while fixing L at 0.58D. Figure 12 shows how the jet deflection angle varies with $<c_\mu>$ for the three diffusers. Clearly, the ø=15˚ diffuser is the least effective of the three. The differences between the ø=22.5˚ diffuser and the ø=30˚ diffuser are small, but the ø=30˚ diffuser appears to be the most effective over the range of parameters tested. The mean velocity profiles, shown in Figure 13, indicate that the ø=15˚ diffuser is less effective at entraining the flow on its upper side than the ø=22.5˚ and ø=30˚ diffusers. It also deflects the jet less. The turbulence levels of the ø=15˚ diffuser are higher than the other two diffusers (not shown). This is true for both shear-layers. The differences between the U and u' profiles for the ø=22.5˚ and 30˚ diffusers are small, but still higher deflection angles as well as larger turbulence levels at the jet core were obtained using the diffuser with a 30˚ half-angle.

3.3.5 The effect of the excitation direction

It is well known that when linear stability is valid and low amplitude excitation is used, the method of excitation is not important. At a certain distance from the source, typically a few wavelengths downstream, the excitation will be independent of the source details. On the other hand, when high amplitude excitation is considered, and non-linearity plays an essential role, the source characteristics could dominate. This is especially important when the whole interaction length between the controlled jet and the diffuser is about five wavelengths long. Two extreme options for the relative direction between the excitation and the jet flow direction were considered. The excitation was introduced in either the streamwise or cross-stream direction. As already shown in Figures 6c and 6f, the high amplitude cross-stream excitation deflects the jet away from the excitation slot. This causes the jet cross section to be elongated along the z-axis rather than along the y-axis. This type of excitation does not enhance the spreading rate nor does it elevate the turbulence levels as much as the streamwise excitation.

Figure 14 shows jet deflection angles versus $<c_\mu>$ for streamwise (X-diffuser and no diffuser) and cross-stream (R-diffuser) excitations. For small $<c_\mu>$'s, the jet is deflected in the same direction (upward) for both types of excitation with a diffuser present. The introduction of low $<c_\mu>$ excitation into the upper shear-layer causes enhanced spreading and interaction of that shear-layer with the diffuser wall. As the level of $<c_\mu>$ increases, the streamwise (X-diffuser) introduction of periodic momentum continues to gradually deflect the jet upward, towards the excited shear-layer, while the jet is deflected downward when using cross-stream excitation (R-diffuser) with $<c_\mu>$ greater than 0.5%. Note that for both the X-diffuser and the R-diffuser the excitation is introduced through the slot surrounding the upper quarter of the jet circumference. Figures 15a and 15b show a comparison of the mean and turbulence velocity profiles for the baseline and controlled ($<c_\mu>$~ 3%) jet using the X-diffuser, the R-diffuser, and without a diffuser present. The effect of introducing the excitation in the streamwise direction without a diffuser is to increase the spreading rate of the excited shear-layer (Fig. 15a and 15b). This was accompanied by significantly smaller jet deflection angles, compared to the deflection angles found for the X-diffuser (Fig. 14). The X-diffuser causes enhanced spreading on the side of the excited shear-layer that interacts with the diffuser wall to deflect the entire jet to that side (Fig. 15a). High level $<c_\mu>$, introduced in the cross-stream direction (R-diffuser), deflects the jet very effectively towards the opposite diffuser wall, without enhancing its spreading rate in a comparable manner (see also Fig. 6c and 6f). This might be important from an application point of view.

3.4 The response of the jet to pulsed excitation

A wave packet is generated when a strong and concentrated disturbance, in both space and time, is introduced into an unstable shear-layer. The concentrated excitation produces a complete spectrum of disturbance modes. The unstable shear-layer will selectively amplify the most unstable modes and dampen the rest. This approach was first introduced by Gaster[16] to study linear instability of the Blasius boundary layer. It was later applied to free-shear layers by Balsa[17]. Very good agreement between linear stability theory and experiments was found in the initial stages of transition. Further

downstream, various modes interact to promote breakdown. Gaster, et. al.[18] demonstrated that linear stability theory could be applied to predict the evolution of two-dimensional harmonic wave trains introduced into a turbulent shear-layer. The interaction between the linearly unstable modes and random turbulence could also be incorporated using an eddy viscosity model to improve the agreement between theory and experiment[19]. Once the magnitude of the excitation is strong enough (at least 1% of the reference velocity), linear theory fails to predict the evolution and non-linearity dominates the evolution of the disturbance[20]. In transitional boundary layers this type of excitation generates turbulent spots and in pipe flow it generates puffs and slugs. Zilberman et. al[21] used an electric spark excitation to generate a turbulent spot and study its evolution in a fully turbulent boundary layer. A similar approach is presently used to study the frequency content, the effect of the excitation direction, the disturbance convection speed and the relationship between the excitation and the non-linear instability mechanism.

The results presented thus far clearly demonstrate that periodic excitation could be used to vector a turbulent jet and enhance its spreading rate. The results of the parameter study indicate that the jet deflection angle is only weakly affected by F^+ and Re_D. The diffuser half-angle, diffuser length, and excitation direction have a strong effect on the evolution of the jet. It was also demonstrated that the presence of the diffuser has a strong effect on the effectiveness of the streamwise excitation. Wave packet studies were performed to understand how periodic excitation interacts with the jet flow and with the diffuser. A wave packet was generated by introducing a single cycle of the 700Hz excitation, through the slot surrounding the upper 90˚ of the jet circumference. The actuator and the data acquisition sequence were triggered simultaneously. The data were sampled at 6 KHz and 2500 records containing 512 points were acquired at each measurement station. The large number of data records were needed because of the low ratio between the wave packet signal and the background turbulence. Data were acquired for two different excitation input levels that differed by about a factor of two in the amplitude of the pressure fluctuations, as measured in the actuator cavity. Data were acquired in the jet upper shear-layer, where $U/U_e = 0.75$, at six axial locations, x/D=0.1, 0.2, 0.4, 0.8, 1.2, 1.6, inside the diffuser (when present). This was repeated three times using the X-diffuser, the R-diffuser and without a diffuser. Even though 2500 realizations were ensemble averaged, the low amplitude wave packet signal is hardly detectable (not shown). However, with the diffuser present, the wave packet generated by the streamwise excitation is amplified and detectable. Figures 16a, 16b and 16c show the jet response to the high amplitude pulsed excitation. Note that the data signal are separated by u'/Ue=0.05 for clarity. The resulting wave packet is clearly seen for all three jet exit configurations. For x/D=0.1 and 0.2 and time, t< 6msec, the signals are identical showing the response to the one cycle 700Hz pulse. Further downstream, the amplitude of the wave packet generated by streamwise excitation (X-diffuser Fig. 16b) is the highest of all three cases. The wave packet, generated in the absence of a diffuser (Fig. 16a), appears sooner at the measuring station and has only weak negative velocity perturbations in front of it. The cross-stream (R-diffuser) excited wave packet (Fig. 16c) is the least amplified of the three cases. The amplitude of the wave packet as a function of x was computed by integrating the time histories shown in Figures 16. The amplitude, Amp, is expressed in terms of total fluctuating momentum in the form

$$Amp = \int_{t=0}^{t=50\,msec} \frac{u'^2}{U_e^2}\,dt \qquad \text{(Eq.6a)},$$

where the velocity perturbation, u'(t), is given by

$$u'(t) = U(t) - \frac{1}{T}\int_{t=50\,msec}^{80\,msec} U(t)\,dt \qquad \text{(Eq. 6b)},$$

and the integration period, T, is 30msec, after the response to the wave packet has passed. The times of integration were chosen because the flow returns to its undisturbed state at about t=50 msec as shown in Figures 16. Integrating the perturbation momentum beyond this point would only add noise. The total fluctuating momentum of the wave packet can also be viewed as a magnitude of the mean flow distortion. Figure 17 shows how the total fluctuating momentum of the wave packet varies with x for the three jet exit configurations examined. The initial fluctuating momentum is identical for the three configurations, indicating that the input is not sensitive to the presence of the diffuser or to the excitation direction. Figure 17 clearly shows that the disturbance resulting from the pulsed excitation in the streamwise direction (X-diffuser) is the most amplified. A factor of about two in the ratio of the integrated fluctuating momentum is seen between the X-diffuser and the no diffuser wave packet. This ratio increases to almost three at x/D=1.6. The disturbance resulting from the cross-stream excitation is the least amplified of the three configurations. Further analysis, experimentation, and theoretical considerations are needed to clarify the physical

mechanism leading to these differences. Figure 17 also shows the *Amp* values integrated across the entire y range. The ratio of about three between the R- and X- modes indicates that the results presented in Figure 17 for U/U_e=0.75 are of a global nature.

Wave Packet surveys were also made at x/D=1.6, the diffuser exit, using the X-diffuser (Fig. 18a) and the R-diffuser (Fig. 18b) across the entire y range of the jet at its plane of symmetry, z/D=0.0. The wave packet generated by streamwise excitation (X-diffuser) is of significantly higher amplitude in the excited shear-layer than in the non-excited layer (3% and 0.5% respectively). The cross-stream excitation (R-diffuser) affects the entire jet cross-section, generating comparable amplitudes in both shear-layers. The maximum amplitude of the X-diffuser wave packet is much higher than the maximum amplitude of the R-diffuser wave packet. This demonstrates how much more receptive the excited shear-layer is to streamwise excitation. It also shows that the cross-stream excitation generates a more global response rather than the response generated by the streamwise excitation. This pattern clarifies why the jet is effectively vectored towards the excited shear-layer side when using the X-diffuser (Fig. 14). It also indicates that the excitation using the R-diffuser is not related to an instability mechanism when high amplitude is applied, but does not reveal the reason why it is effectively deflected to the opposite direction. The mechanism responsible for the jet deflection away from the excitation slot, using the R-diffuser, is similar to the mechanism responsible for the modification in the jet cross-section measured by Davis[3] using two steady control jets.

The convection speeds of the wave packet (Fig. 19) were computed by determining the wave packet appearance time at each x location for the three types of high amplitude excitation. The wave packet was thought to be in the initial stages of development at x/D=0.1 and 0.2, therefore these two points were omitted from the convection speed computations. All convection speeds were calculated by applying a linear fit to the data shown in Fig. 19. The convection speeds are around 60% of the jet exit velocity. This value corresponds favorably with convection speeds of coherent structure in turbulent shear-layers[21], and with linear stability theory predictions (Ref. 15 and references therein). The convection speed of the wave packet generated by streamwise excitation (X-diffuser) is slightly higher, even though the mean flow speed is lower when the jet is spread more towards the excitation slot. This indicates that this mode of excitation should result in faster response to changes in the excitation $<c_\mu>$. The reason for the earlier appearance of the wave packet when there is no diffuser at the jet exit is not clear. It might be connected to slight differences in the nature of the interaction between the excitation and the shear-layer very close to the excitation slot, in the absence of the diffuser

Analyzing the frequency content of the wave packet reveals that the most amplified frequency for the free jet (no diffuser attached) is around 100 Hz. This frequency corresponds favorably with both shear-layer modes[15], $S_{t\theta}$=0.02, and with the column mode, S_{tD}~0.2-0.6. However, the limited frequency scans performed (Fig. 9) indicate that the 300Hz excitation did not generate higher deflection angles than the 700Hz excitation in the range of parameters studied. The most amplified frequency is reduced to 50-70Hz when the X-diffuser and R-diffuser are used. These frequencies combined with a convection speed of $0.6U_e$ result in a disturbance wavelength of about 3 jet diameters. It seems that this wavelength is too long to interact with a diffuser that is about half this length. It remains to be seen if longer diffusers and lower frequencies will be more effective.

3.5 Jet response to step changes in $<c_\mu>$

3.5.1 General

The response of the flow to step changes in the magnitude of the excitation, $<c_\mu>$, was also investigated. Studying the response of a system is a fundamental step in identifying the dynamics of the control process. For this investigation, data were acquired with the actuator toggled between off, on and off again. Data acquisition and the initial actuator on command were triggered simultaneously. For each flow condition, 512 records, containing 6000 data points acquired at 12KHz, were ensemble averaged. The excitation was again introduced through the slot surrounding the upper 90˚ of the jet circumference, and the frequency of the excitation when the actuator was on was 700Hz. All measurements were made at an axial location corresponding to the diffuser exit, x/D=1.6 and the plane of symmetry of the excitation, z/D=0.0. In the cases where a diffuser was attached to the jet exit, the length of the diffuser, L, was 1.85D and the half-angle, ø, was 30˚.

3.5.2 Effect of the excitation direction

The effect of the excitation direction on the jet response was studied at $Re_D=3.1x10^4$ resulting in an F^+=4.2 when a diffuser was present. The $<c_\mu>$ when the actuator was on was 1.6% and 2.2% for cross-stream (R-diffuser) and streamwise (X-diffuser and no

diffuser) excitation, respectively. Such a variation in $<c_\mu>$ should not have a significant effect on the results since measurements acquired for different $<c_\mu>$ levels did not lead to changes in the transient jet flow response when normalized by the steady-state jet flow conditions. The hot-wire was positioned in the excited shear-layer, at a y location corresponding to $U/U_e=0.50$, $y_{0.5}$. Figures 20a and 20b show the ensemble-averaged velocities, normalized by the jet exit velocity. At time t=0.0 the actuator is switched on. It operates for 0.49 seconds before being switched off. The on and off times of the actuator have been subtracted to align the on and off times at t=0. The abscissa of Fig. 20a and 20b has the actuator toggle time multiplied by the convection speed determined in Section 3.4, producing a response convection length. This length scale, U_c*time, is normalized by the jet diameter, D, relating the jet response time to distance in terms of jet diameters. When control is switched on, the flow responds in a matter of milliseconds to the change in $<c_\mu>$ in all cases. The response of the jet to switching the streamwise excitation on without a diffuser attached is the fastest, in agreement with the wave packet convection results shown in Figure 19 and with the higher frequency content of that wave packet. Switching the streamwise excitation (no diffuser and X-diffuser) on results in an initial vectoring of the jet below the baseline state followed by an upward deflection of the jet above the controlled state before converging to the controlled steady-state. The jet response to switching the cross-stream excitation (R-diffuser) on is smoother but is the slowest among the three cases studied. The jet response to switching the streamwise excitation off, in the absence of a diffuser (Fig. 20b), is the fastest and is accompanied by a slight deflection above the controlled steady-state. The jet response to switching the cross-stream excitation off is smooth, fast and is accompanied by only a small deflection above the baseline state before converging to the baseline steady-state. Figure 20b indicates that the jet response to turning the streamwise excitation off (X-diffuser), is initially accompanied by a deflection higher than the controlled steady-state at 2D and a deflection lower than the baseline steady-state centered around 4.5D. The effect of different diffuser lengths on the response of the jet to step changes in the excitation level has not been studied yet. Looking at the normalized response times, the jet starts to respond at a convection distance of about 2D and the transition stage also takes about 2D-4D (Fig. 20).

Measurements were also made over the entire center plane of the jet, at x/D=1.6, to assess the overall response of the jet to a step change in $<c_\mu>$. Figure 21 presents the jet response to on-off excitation in the form of mean velocity contours normalized by the jet exit velocity using streamwise (X-diffuser) and cross-stream (R-diffuser) excitation. For both types of excitation, the jet starts to respond at about 10 msec from the step change in $<c_\mu>$. The jet response to switching the streamwise excitation on is initially characterized by a strong downward deflection (below the baseline steady-state) that is followed by an upward deflection (above the controlled steady-state) of the excited shear-layer (Fig. 21a), before converging to the controlled steady-state. This response could be interpreted as the shedding of a counter clockwise rotating vortex from the upper shear-layer as a response to turning $<c_\mu>$ on. The opposite happens when the streamwise excitation (X-diffuser) is turned off (Fig. 21b). The excited shear-layer starts to bend upward immediately, resulting in an even higher upward deflection at about 10 msecs after $<c_\mu>$ has been turned off, and a small deflection below the baseline state at 24 msec. This response could be interpreted as the shedding of a clockwise rotating vortex from the upper shear-layer. The opposite shear-layer responds more smoothly, but both shear-layers have deflections below the baseline steady-state at about 20 to 24 msec.

The transients of the jet response, to turning on the cross-stream excitation (R-diffuser Figure 21c), are smoother throughout the center plane (Fig. 21c). Unlike the smooth response seen for switching the cross-stream excitation (R-diffuser) on, the transient stage of the jet response to switching the cross-stream excitation (R-diffuser) off begins with a slight vectoring of the jet below the controlled state followed by a vectoring of the jet above the baseline state before gradually reaching the baseline steady-state.

The transient responses described above could be interpreted as vortices shed from the jet exit as the excitation is turned on and off. An upward deflection is accompanied by a shedding of a counterclockwise vortex while a downward deflection is accompanied by a clockwise vortex. It seems that the on response of the streamwise excitation and the off response of the cross-stream excitation generate more concentrated vortices. More direct measurements of vorticity are required to validate this hypothesis.

3.5.3 The effect of jet exit velocity

The Reynolds number dependence of the response was studied by altering the jet exit velocity and repeating the tests described in Section 3.5.2

using streamwise excitation (X-diffuser). The results for Reynolds numbers corresponding to U_e=8, 12 and 18 m/s are presented in Figures 22a and 22b for actuator on and off responses, respectively. The $<c_\mu>$ when the actuator was on was 2.4% for all Re_D's. Time is multiplied by U_e to provide a common convection length for the response. This normalization collapses the data very well, indicating Re_D insensitivity and a typical response time of $0.4/U_e$ for the present geometry. Assuming that the convection speed is independent of Re_D, and looking back at Figure 20a and 20b, it is safe to assume that the jet will respond within a convection distance of about 3-4 diameters regardless of Re_D, jet diameter, and its exit velocity.

The fast response and its independence of Re_D are very encouraging for control purposes. However, the strong transients identified in the jet response, mainly of the streamwise excitation are a concern from an application point of view. This is especially important since the streamwise excitation is the most effective as it requires the minimum $<c_\mu>$ to generate effective spreading and vectoring, at $<c_\mu>$ levels of about 1%. This is probably the upper limit of what can be achieved in high subsonic speed applications.

4. Summary and Conclusions

Periodic excitation was introduced through a slot surrounding the upper quarter of the circumference of a circular jet to vector it and enhance its spreading rate. A diffuser, attached to the jet exit, promoted attachment of the jet shear-layer to the diffuser wall in a similar manner to that found in airfoil experiments using periodic excitation.

The boundary layer upstream of the jet exit was tripped to achieve turbulent flow at the jet exit. Data were acquired for Re_D between $1.6x10^4$ and $4.7x10^4$. The tripped boundary layers of the jet generated a Reynolds number independent flow, the desired effect. The turbulence level in the jet core was 3%.

The use of periodic excitation and a diffuser at the jet exit in a flow control experiment introduced additional parameters such as frequency, excitation momentum and its direction, diffuser length, and diffuser half-angle. The jet deflection angles were insensitive to the excitation frequency, in the range of parameters studied. The jet deflection angles were independent of the Reynolds number, although some differences were noticed in the jet behavior when at $Re_D=2.1x10^4$, close to the transition Re_D. Diffusers of length to diameter ratio between 0.58 and 1.85 were tested. The longest diffuser, L/D=1.85, generated somewhat higher deflection angles. Jet deflection angles were lower for a diffuser half-angle of 15˚ than for diffuser half-angles of 22.5˚ and 30˚. Jet deflection was highly sensitive to the direction in which the excitation was introduced. Periodic excitation, introduced in the streamwise direction, vectored the jet towards the diffuser wall where the excitation was introduced. Low amplitude excitation introduced in the cross-stream direction vectored the jet in the same direction, but high amplitude excitation introduced in the cross-stream direction vectored the jet away from the wall where the excitation was introduced.

Pulsed excitation was used to generate wave packets in the jet shear-layer in order to study the frequency content, the effect of the excitation direction, the disturbance convection speed and the relationship between the excitation and an instability mechanism. These studies revealed that the presence of a diffuser at the jet exit significantly amplified the pulsed excitation introduced in the streamwise direction. The favorable interaction between the excitation, the jet flow and the diffuser wall explains the higher jet deflection angles obtained with the diffuser when exciting the shear-layer in the streamwise direction. The wave packet excited by introducing a pulsed excitation in the cross-stream direction evolved differently even though a diffuser was present. This wave packet is the least amplified among the cases studied. It is also of similar amplitude in both the excited and opposite shear-layers, indicating a more global effect of the excitation when introduced in the cross-stream direction. This is consistent with the jet being deflected towards the opposite diffuser wall when using high amplitude cross-stream excitation.

The jet responded quickly, on the order of 10-20 milliseconds, to step changes in the level of the excitation. The response was independent of the Reynolds number when the jet exit velocity was increased. The practical implication of this finding is that a proportional increase in dimensions and speed will maintain a similar response time. The jet response to turning the excitation on is quicker, when the excitation is introduced in the streamwise direction, than when it is introduced in the cross-stream direction. However, this is accompanied by stronger transients, similar to an underdamped system. These transients can also be interpreted as shedding of a vortex whenever a step change in the level of the excitation occurs. The sign of the vortex is determined by the direction of the resulting jet deflection.

From this jet control study, a number of areas for future research were identified. One area is the use

of simultaneous streamwise and cross-stream excitation on opposite sides of the jet. It is assumed that significantly higher jet deflection angles could be obtained this way. The effect of the diffuser on the cross-stream excitation has not been studied yet. More wave packet studies, where diffusers of different lengths would be used, are required to better understand how the amplification and convection speed of the wave packet (and the associated mean flow distortion) are effected by the diffuser length. Finally, it is planned to use periodic excitation for the control of a rectangular jet with an exit diffuser. A rectangular jet is of interest because of the longer shear-layers per unit area and the additional possible modes. One such mode is jet rotation.

A fast responding method of altering the direction of the flow emanating from a low speed, turbulent circular jet was demonstrated. Moderate $<c_\mu>$'s were required to produce this effect. The technique could be applied to a number of applications including, jet engine exhaust, gust alleviation, and control surface augmentation or replacement without moving parts.

Acknowledgment

This work was performed while the second author held a National Research Council - NASA LaRC research associateship. The authors would like to thank Mr. W. L. Sellers III, Mr. M. Walsh, Dr. R. Joslin and Ms. C.B. McGinley for their support.

References

1) Crow, S. C. and Champagne, F. H., "Orderly Structure in jet turbulence", *Journal Of Fluid Mechanics* Vol. 48, part 3, 1971, pp. 547-591.
2) Zaman, K.B.M.Q, and Hussain, A.K.M.F, "Turbulence suppression in free shear flows by controlled excitation", *Journal of Fluid Mechanics*, Vol. 103, 1981, pp. 133.-159.
3) Davis, M.R., "Variable Control of Jet Decay", *AIAA Journal*, Vol. 20, No. 5, 1982.
4) Strykowski, P. J. and Wilcoxin, P. J., "Mixing enhancement due to global oscillations in jets with annular counterflow", *AIAA Journal*, Vol. 31, No. 3, March 1993.
5) Strykowski, P.J. and Krothapalli, A., "The Countercurrent Mixing Layer: Strategies for Shear-Layer Control", AIAA paper 93-3260, 1993.
6) Strykowski, P.J., Krothapalli, A., and Forliti, D. J., "Counterflow Thrust Vectoring of Supersonic Jets", AIAA paper 96-0115, 1996
7) Raman, G. and Cornelius, D., "Jet Mixing Control using Excitation from Miniature Oscillating Jet", *AIAA Journal*, Vol. 33, No. 2, 1995
8) Smith, B. L., and Glezer, A., "Vectoring and Small-Scale Motions Effected in Free Shear Flows Using Synthetic Jet Actuators", AIAA paper 97-0213, 1997
9) Huerre, P. and Monkewitz, P. A., "Absolute and convective instabilities in free shear layers", *Journal of Fluid Mechanics* Vol. 159, 1985, pp. 151-168.
10) Seifert, A., Bachar, T., Koss, D., Shepshelovich, M. and Wygnanski, I., "Oscillatory Blowing, a Tool to Delay Boundary Layer Separation", *AIAA Journal*, Vol. 31, No. 11, 1993, pp. 2052-2060.
11) Seifert, A., Darabi, A. and Wygnanski, I., "On the delay of airfoil stall by periodic excitation", *Journal of Aircraft*, Vol. 33, No. 4, 1996, pp. 691-699.
12) Seifert, A. and Pack, L.G., "Oscillatory Control of Separation at High Reynolds Numbers", AIAA paper 0214-98, 1998.
13) Kinser. E. and Rediniotis, O.K., " Development of A Nearly-Omni-Directional, Three-Component Velocity Measurement Pressure Probe," AIAA paper 96-0037, 1996.
14) Husain, Z.D. and Hussain, A.K.M.F, "Axisymmetric Mixing Layer: Influence of the Initial Boundary Conditions", *AIAA Journal*, Vol. 17, No. 48, 1979.
15) Drubka, R. E., Reisenthel, P., Nagib, H. M., "The dynamics of low initial disturbance turbulent jet", *Physics of Fluids*, A 1 (1), 1989, pp. 1723-1735.
16) Gaster, M., "The development of three-dimensional wave packets in a boundary layer", *Journal of Fluid Mechanics*, Vol. 32, 1968, pp.173-184.
17) Balsa, T.F., "Three-dimensional wave packets and instability waves in free shear layers and their receptivity", *Journal of Fluid Mechanics*, Vol. 201, 1989, pp. 77-97.
18) Gaster, M., Kit, E., and Wygnanski, I., "Large-scale structures in a forced turbulent mixing layer", *Journal of Fluid Mechanics*, Vol. 150, 1985, pp. 23-39.
19) Tumin, A. and Likhatchev, O., "On Harmonic perturbations in turbulent shear flows", Presented at the 51st Meeting of the APS/DFD, Philadelphia, PA, 1998.
20) Morkovin, M. V., " On the many faces of transition", in Wells, C.S. (ed.), Viscous Drag Reduction, Plenum Press, New York, Sept. 1969, pp. 1-31.
21) Zilberman, M., Wygnanski, I., Kaplan, R.E., "Transitional boundary layer spot in a fully turbulent environment", *Physics of Fluids* Supplement 20 (1977) S258-271.

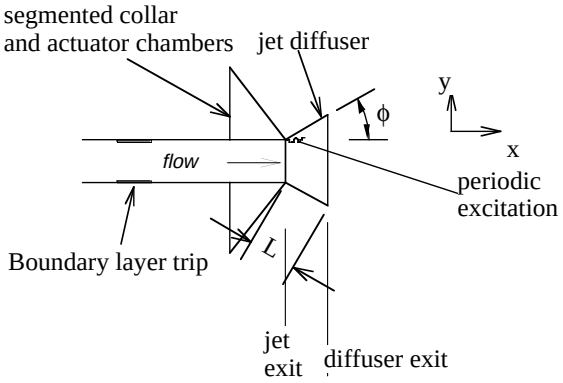

Figure 1a: Schematic of jet side view.

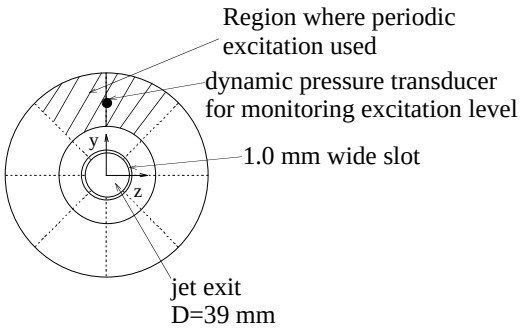

Figure 1b: Schematic of jet front view.

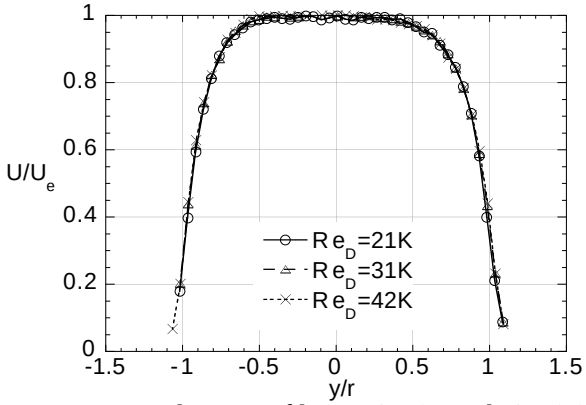

Figure 2a: Baseline U profiles at x/D=0.1 and z/D=0.0.

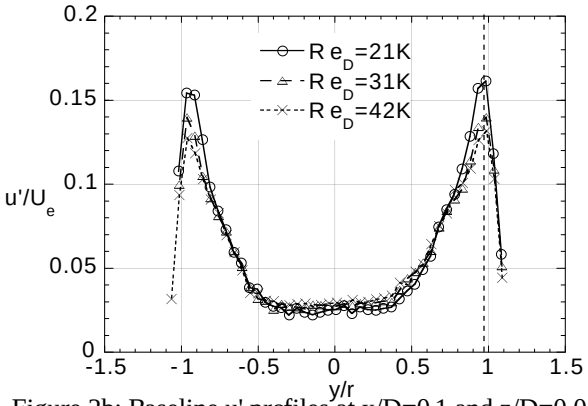

Figure 2b: Baseline u' profiles at x/D=0.1 and z/D=0.0. (Dashed line indicates y location of spectra shown in Figure 3.)

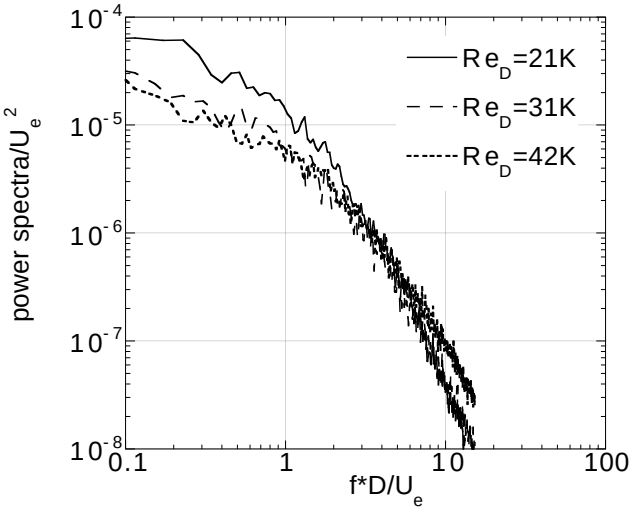

Figure 3: Baseline spectra at y/r=0.97, x/D=0.1.

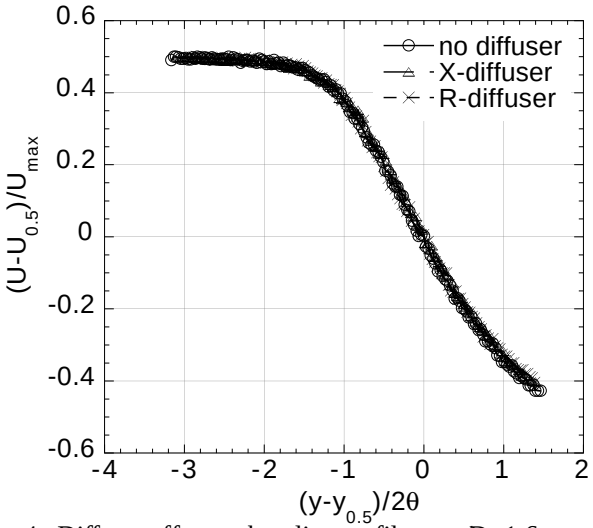

Figure 4 : Diffuser effect on baseline profiles at x/D=1.6, z/D=0.0, Re_D=3.1x10^4. ø=30˚ and L=1.85D.

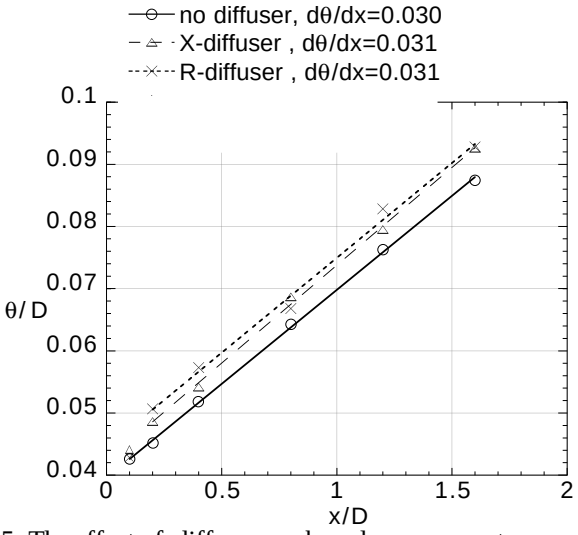

Figure 5: The effect of diffuser on shear-layer momentum thickness close to jet exit. Re_D=3.1x10^4. ø=30˚ and L=1.85D.

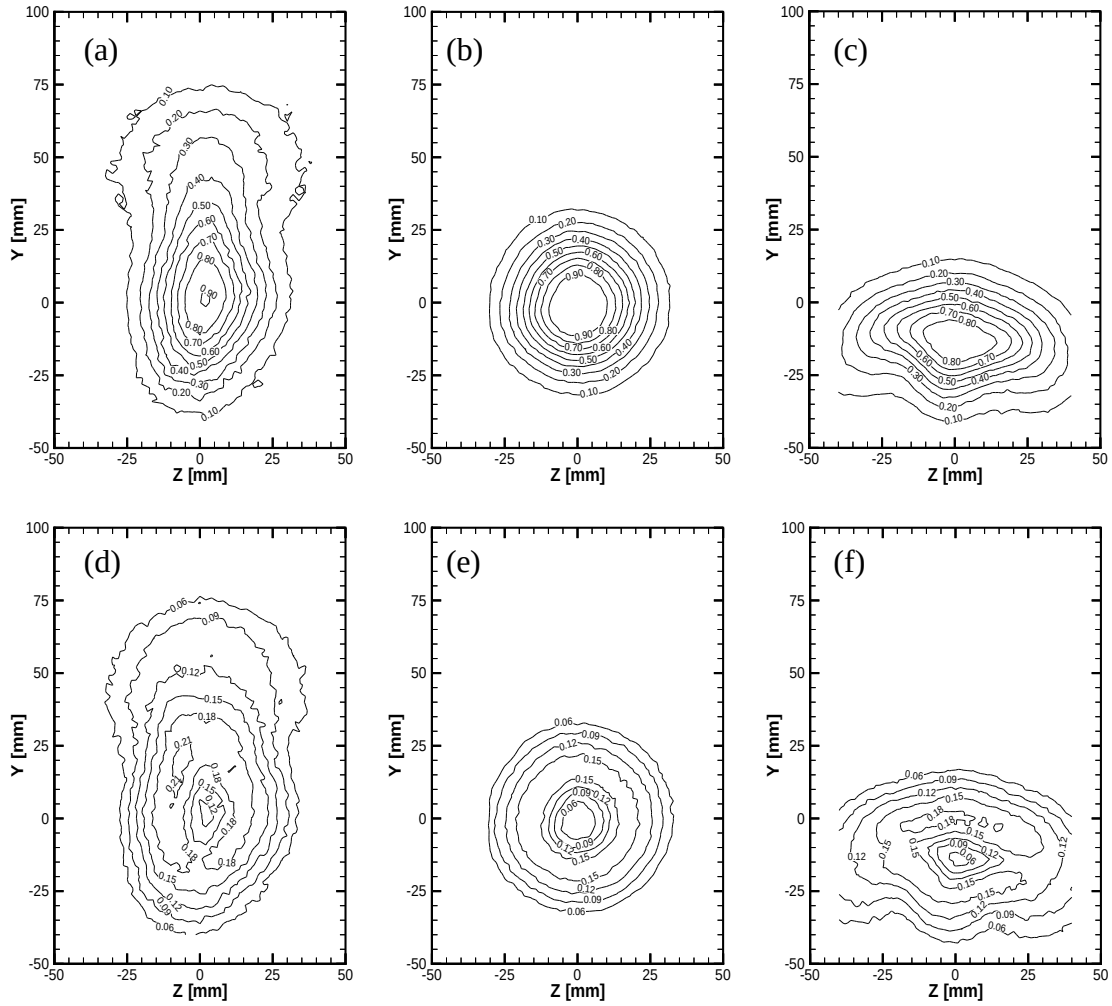

Figure 6: U/U_e and u'/U_e contours at x/D=2.5 $Re_D=3.1x10^4$ for different excitation directions (a) U/U_e, streamwise excitation, $<c_\mu>=3.3\%$, $F^+=2.3$, L=1.0D (b) U/U_e , baseline (c) U/U_e cross-stream excitation $<c_\mu>=3.3\%$, $F^+=4.2$, L=1.85D, (d) u'/U_e, streamwise excitation, $<c_\mu>=3.3\%$, $F^+=2.3$, L=1.0D (e) u'/U_e , baseline, and (d) u'/U_e, cross-stream excitation, $<c_\mu>=3.3\%$, $F^+=4.2$, L=1.85D.

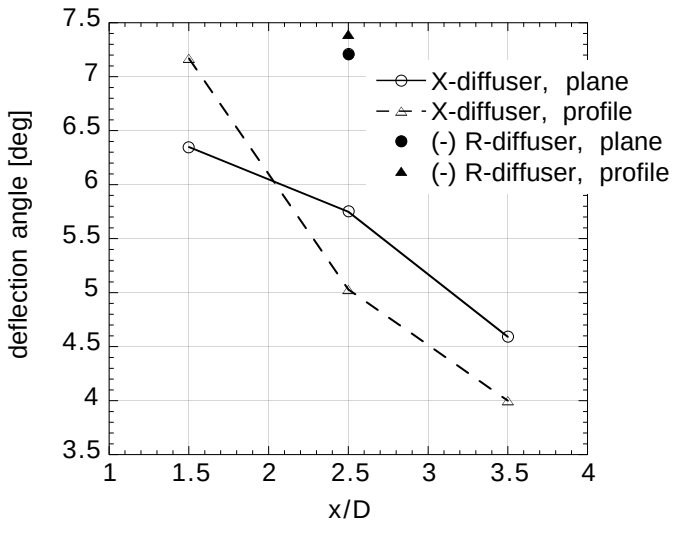

Figure 7: Jet deflection angles computed using profiles on z/D=0.0, and cross-section planes. $<c_\mu>=3.3\%$, $F^+=2.3$, and L=1.0D for X-diffuser. $<c_\mu>=3.3\%$, $F^+=4.2$ and L=1.85D for R-diffuser. $Re_D=3.1x10^4$.

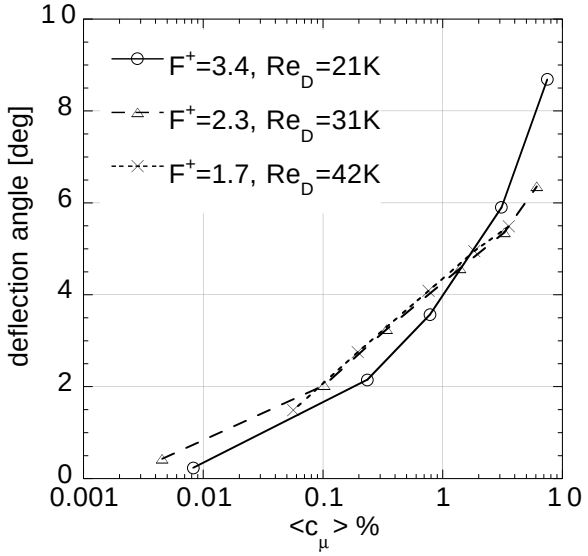

Figure 8: The effect of Re_D on jet deflection angle measured at x/D=2.5 and z/D=0.0 (ø=30˚, L=1.0D X-diffuser).

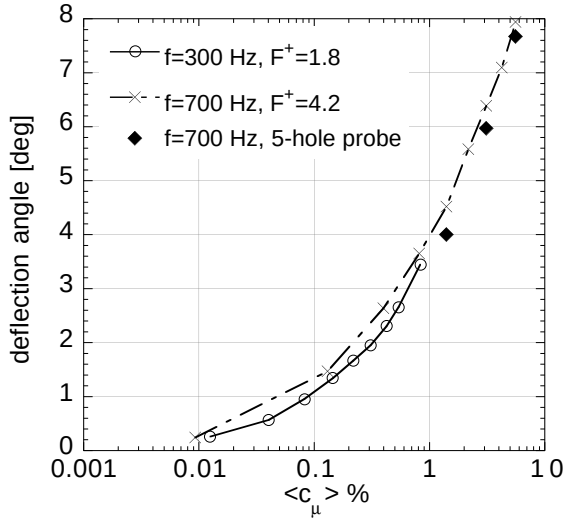

Figure 9: The effect of frequency on jet deflection angles. Re_D=3.1x10^4, x/D=2.5, z/D=0.0, ø=30˚, L=1.85D X-diffuser.

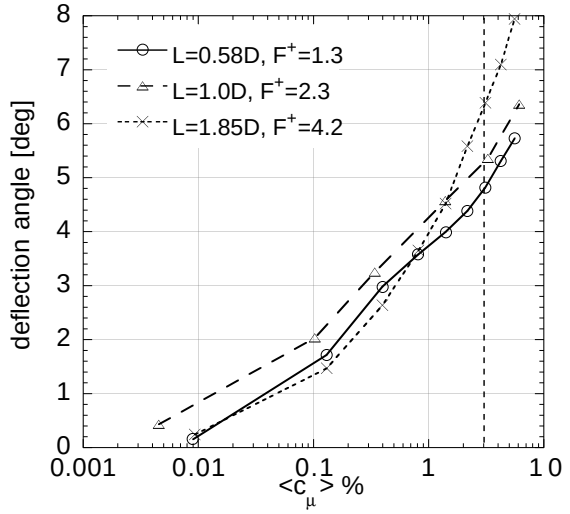

Figure 10: The effect of varying diffuser length , L, on jet deflection angles. ø=30˚ X-diffuser. Re_D=3.1x10^4, x/D=2.5, and z/D=0.0 (Dashed line indicates <c_μ> for profile in Fig. 11).

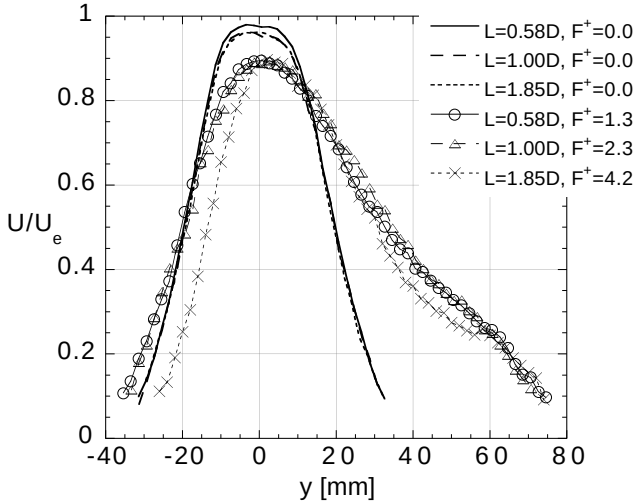

Figure 11: U profiles for varying L. <c_μ>~3% when control applied. ø=30˚ X-diffuser. Re_D=3.1x10^4, x/D=2.5, and z/D=0.0.

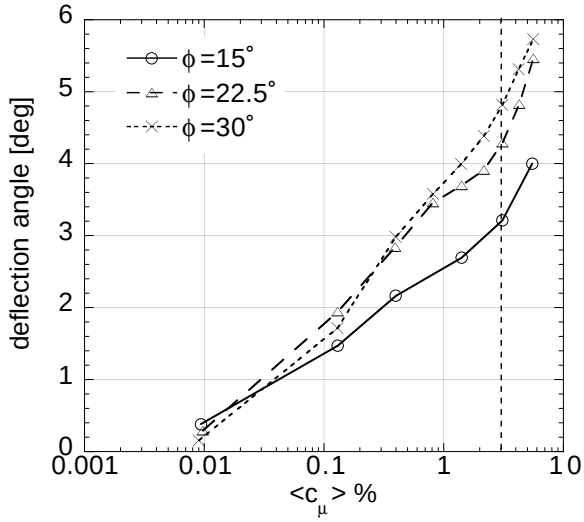

Figure 12: The effect of varying the diffuser half-angle, ø, on jet deflection angle. L=0.58D X-diffuser. Re_D=3.1x10^4, x/D=2.5, z/D=0.0 (Dashed line-profiles in Fig. 13).

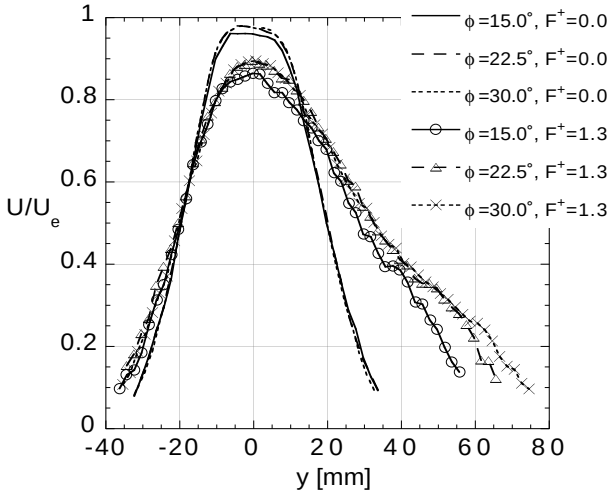

Figure 13: U profiles for different diffuser half-angles, ø, at Re_D=3.1x10^4, x/D=2.5, and z/D=0.0. <c_μ>~3.1% (when control applied). L=0.58D X-diffuser.

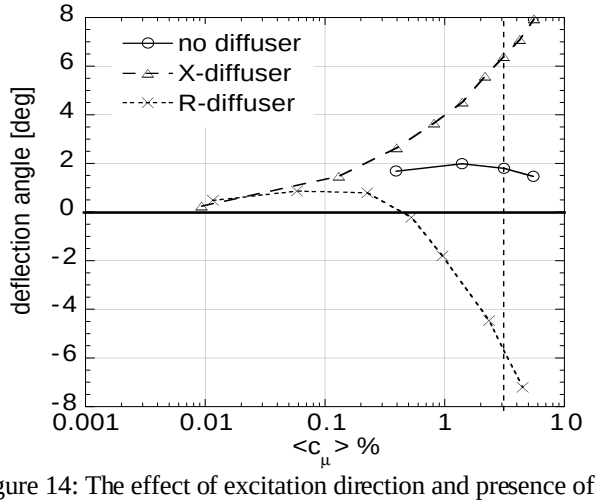

Figure 14: The effect of excitation direction and presence of the diffuser on jet deflection angle. L=1.85D and ø=30˚ (when diffuser present). Re_D=3.1x10^4, x/D=2.5, and z/D=0.0 (Dashed line-profiles in Fig. 15a and 15b).

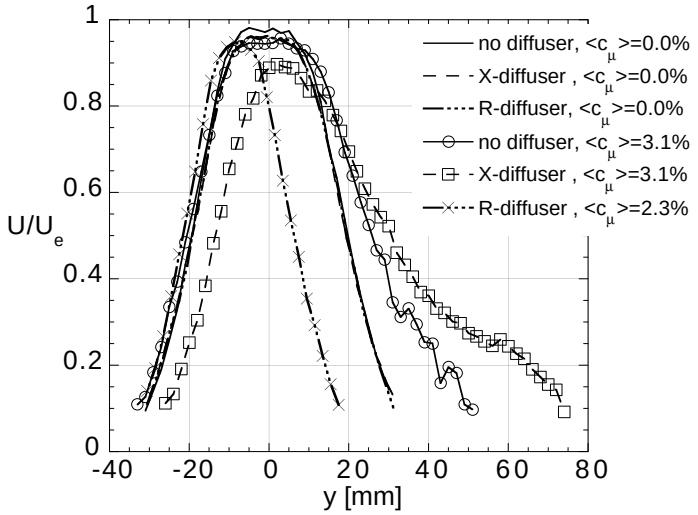

Figure 15a: U profiles showing effect of excitation direction and presence of diffuser on jet. L=1.85D and ø=30˚ (where diffuser present). Re_D=3.1x10^4, x/D=2.5, and z/D=0.0.

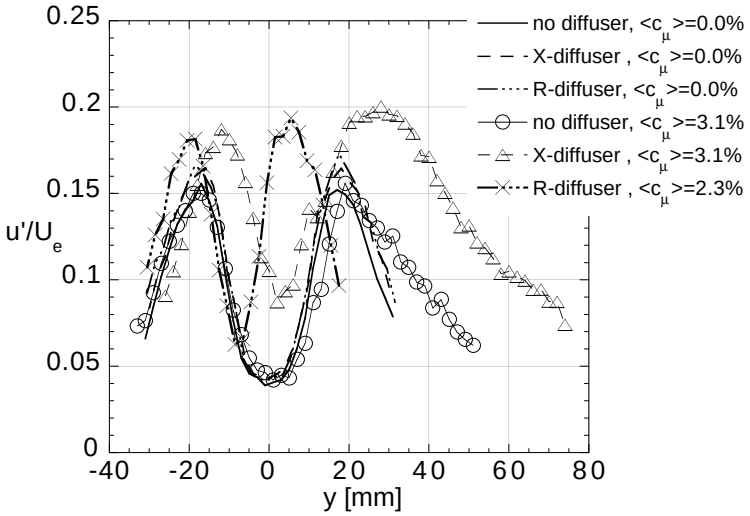

Figure 15b: u' profiles showing the effect of excitation direction and presence of the diffuser on jet. L=1.85D and ø=30˚ (where diffuser present). Re_D=3.1x10^4, x/D=2.5, and z/D=0.0.

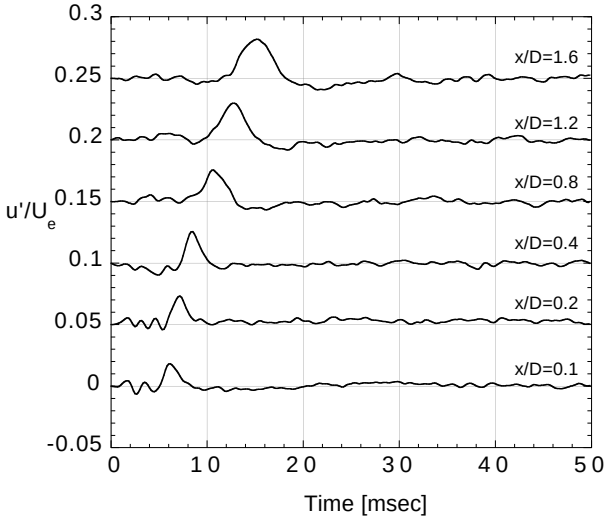

Figure 16a: High amplitude wave packet without diffuser, varying x/D. U/U_e=0.75 and Re_D=3.1x10^4.

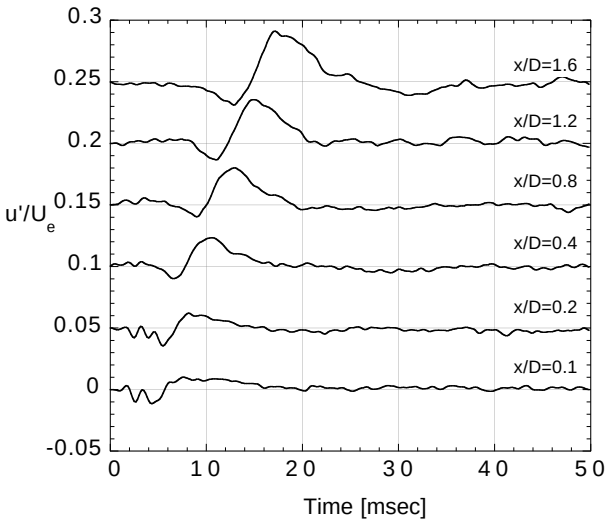

Figure 16b: High amplitude wave packet for X-diffuser L=1.85D, ø=30˚ varying x/D. U/U_e=0.75 and Re_D=3.1x10^4.

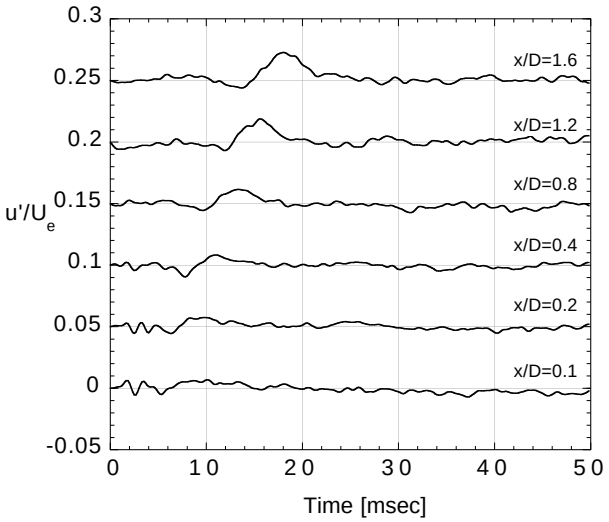

Figure 16c: High amplitude wave packet for R-diffuser L=1.85D, ø=30˚ varying x/D. U/U_e=0.75 and Re_D=3.1x10^4.

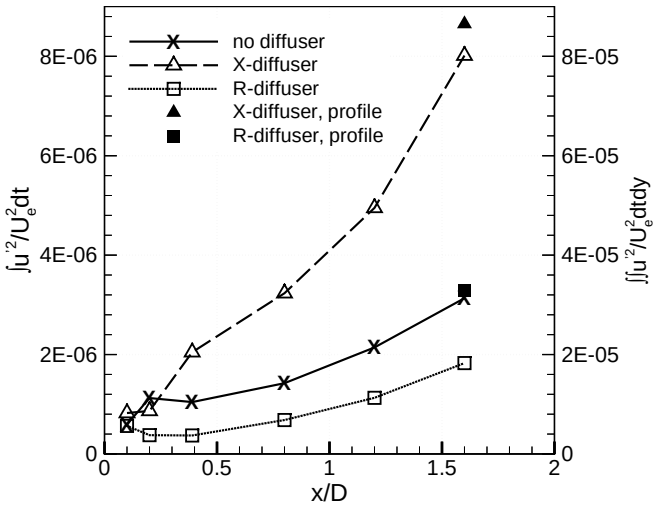

Figure 17: Wave packet amplitudes. Re_D=3.1x10^4.

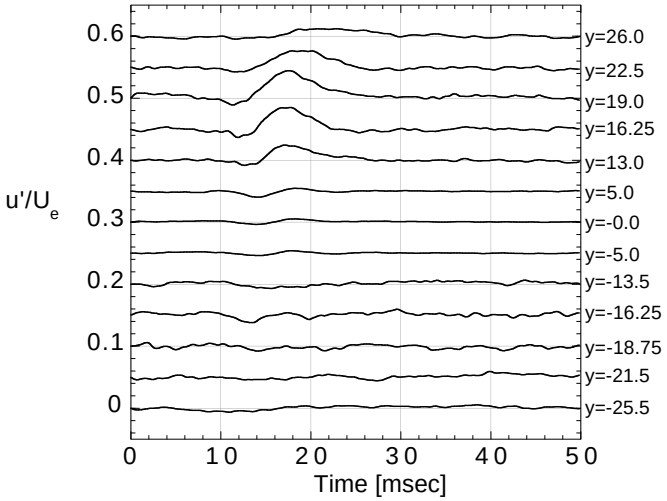

Figure 18a: High amplitude wave packet for X-diffuser L=1.85D, ø=30˚. Re_D=3.1x10^4, x/D=1.6, z/D=0.0.

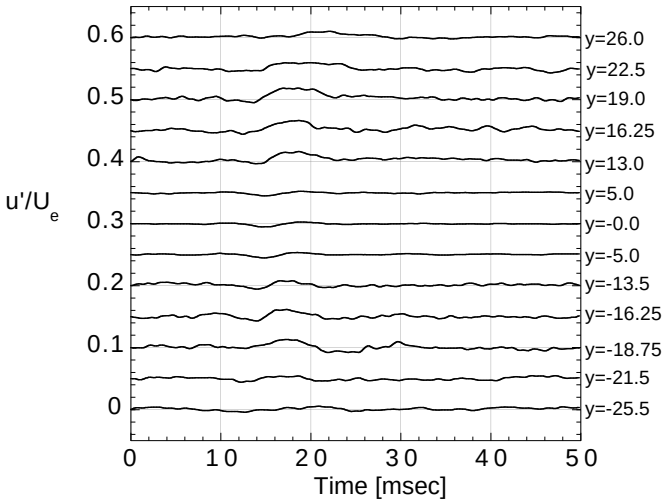

Figure 18b: High amplitude wave packet for R-diffuser L=1.85D, ø=30˚. Re_D=3.1x10^4, x/D=1.6, z/D=0.0.

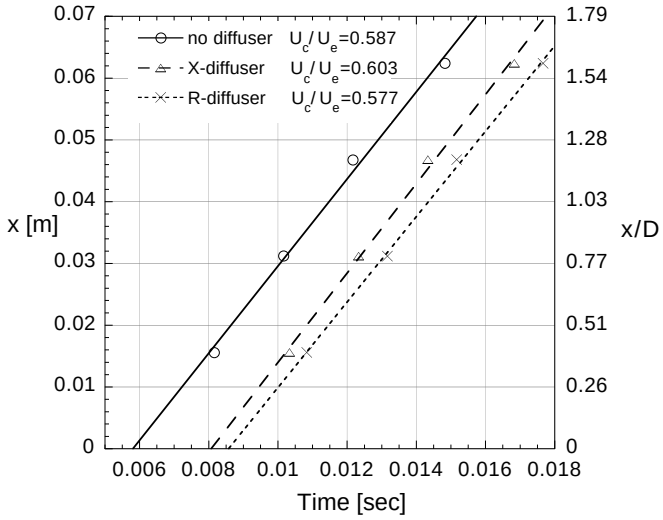

Figure 19: Wave Packet detection time (Conditions specified in Fig. 16).

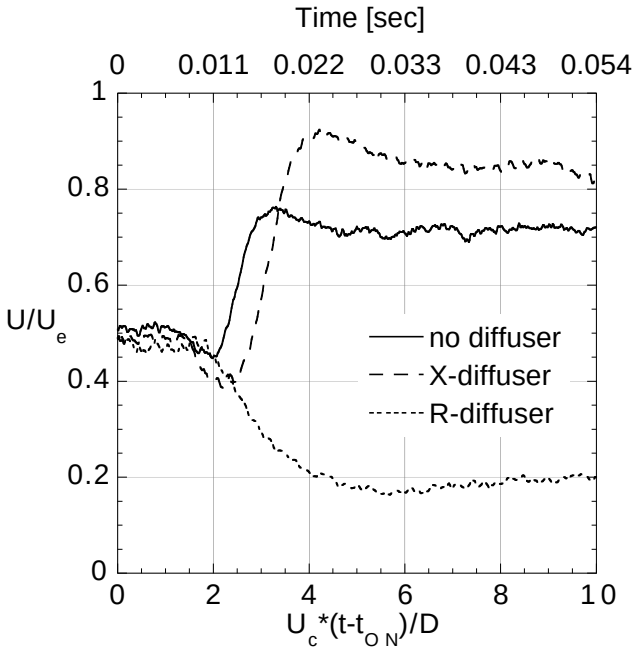

Figure 20a: Effect of excitation direction and presence of diffuser on jet response to a step change in $<c_\mu>$ (0-2.2% streamwise and 0-1.6% cross-stream). Re_D=3.1x10^4. ON.

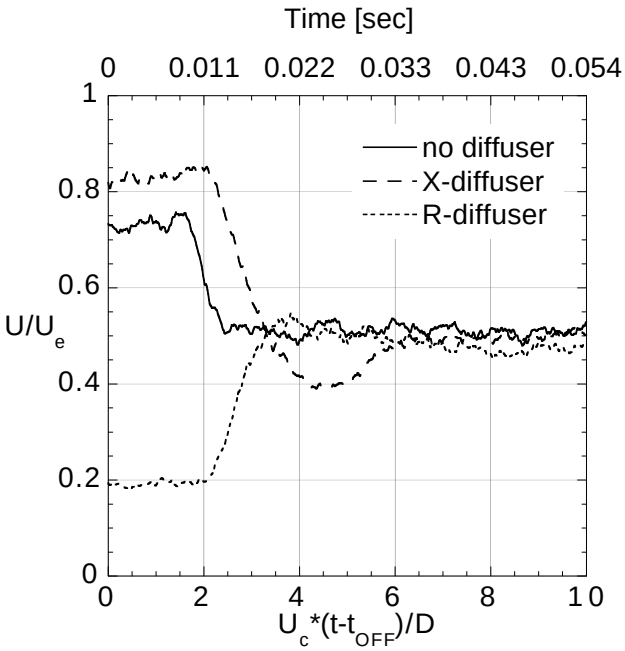

Figure 20b: Effect of excitation direction and presence of diffuser on jet response to a step change in $<c_\mu>$ (2.2 -0% streamwise and 1.6-0% cross-stream). Re_D=3.1x10^4. OFF.

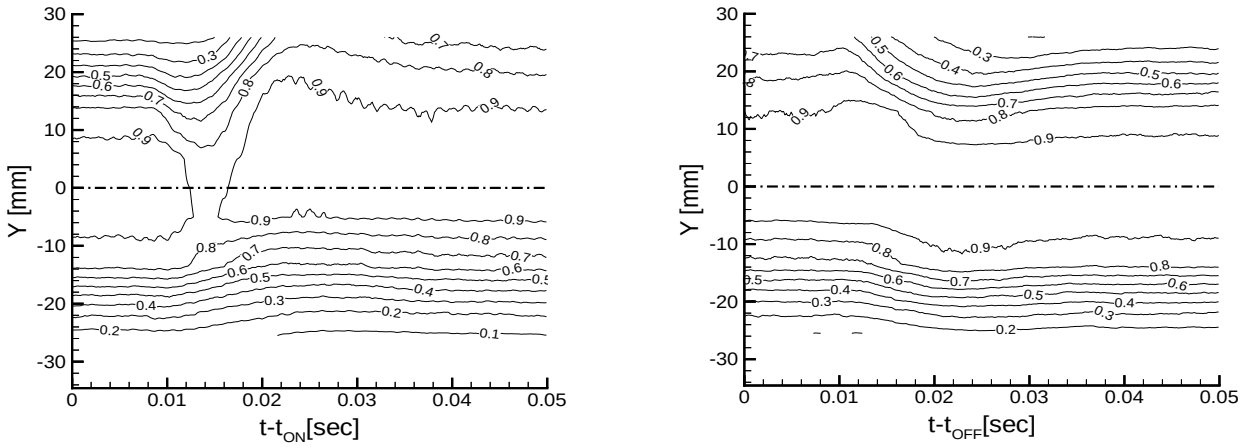

a) X-diffuser, Excitation ON

b) X-diffuser, Excitation OFF

c) R-diffuser, Excitation ON

d) R-diffuser, Excitation OFF

Figure 21: Contours of U/U_e of jet response to a step change in $<c_\mu>$ (0-2.2% for X-diffuser and 0-1.6% for R-diffuser) at $Re_D=3.1x10^4$, x/D=1.6, z/D=0.0 (Dashed-dotted line indicates center of baseline jet).

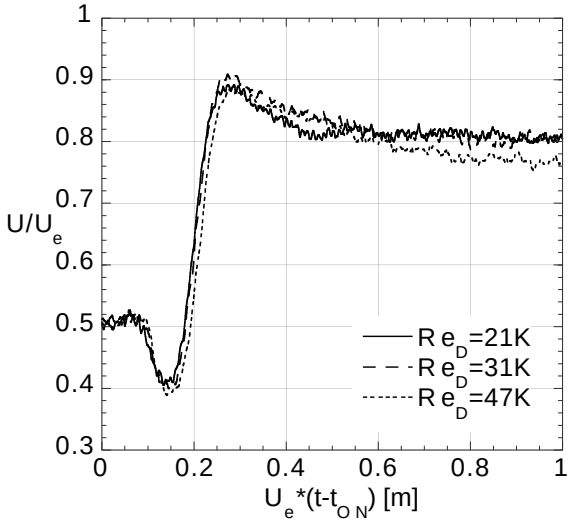

Figure 22a: Effect of Re_D on jet response to a step change in $<c_\mu>$ (0.0-2.4%) at x/D=1.6, z/D=0.0, and U/U_e=0.5. ø=30˚, L=1.85D X-diffuser. ON.

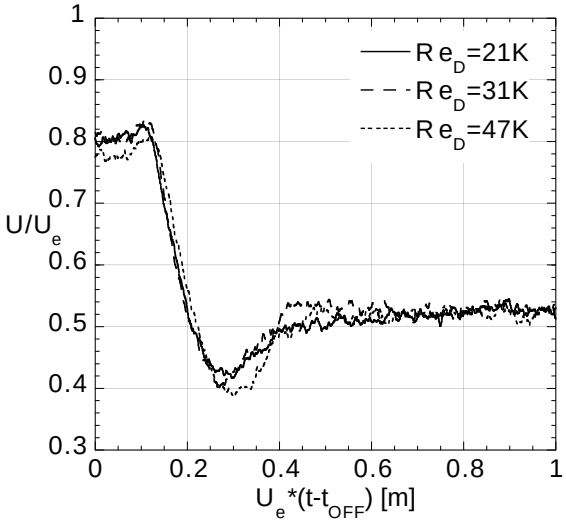

Figure 22b: Effect of Re_D on jet response to a step change in $<c_\mu>$ (2.4- 0.0 %) at x/D=1.6, z/D=0.0, and U/U_e=0.5. ø=30˚, L=1.85D X-diffuser. OFF.